

1 Electrophoresis, Standard Research Articles, Revised

2 **Determination of acid dissociation constants of flavin**  
3 **analogues by capillary zone electrophoresis**

4 Yuki Tanikami,<sup>1</sup> Takuma Tagami,<sup>1</sup> Mayu Sakamoto,<sup>2</sup> Yukihiro Arakawa (0000-0003-  
5 1000-5799),<sup>3\*</sup> Hitoshi Mizuguchi (0000-0003-2396-6812),<sup>3</sup> Yasushi Imada (0000-  
6 0002-4844-5418),<sup>3</sup> and Toshio Takayanagi (0000-0002-5767-1126)<sup>3\*</sup>

7  
8 <sup>1</sup> Graduate School of Advanced Technology and Science, Tokushima University, 2-1  
9 Minamijyousanjima-cho, Tokushima 770-8506, Japan

10 <sup>2</sup> Department of Chemical Science and Technology, Faculty of Engineering,  
11 Tokushima University, 2-1 Minamijyousanjima-cho, Tokushima 770-8506, Japan

12 <sup>3</sup> Graduate School of Technology, Industrial and Social Sciences, Tokushima  
13 University, 2-1 Minamijyousanjima-cho, Tokushima 770-8506, Japan

14  
15 \*Correspondence should be addressed to the following authors:

16 Toshio Takayanagi (Prof.) and Yukihiro Arakawa (Assist. Prof.)

17 Graduate School of Technology, Industrial and Social Sciences

18 Tokushima University

19 2-1 Minamijyousanjima-cho, Tokushima 770-8506, Japan

20 toshio.takayanagi@tokushima-u.ac.jp (T. T.); arakawa.yukihiro@tokushima-u.ac.jp (Y.  
21 A.)

22

23

24 **Keywords:** Acid dissociation constant / Flavin analogues / Instable substances /  
25 Capillary zone electrophoresis

26

27 **Abbreviations:** FL, flavin; RF, riboflavin; LC, lumichrome

28

## 29 **Abstract**

30 Acid dissociation constants ( $pK_a$ ) of 9 kinds of flavin analogues as molecular catalyst  
31 candidates were determined by CZE. Although some of the analogues are instable  
32 and degradable under the light-exposure or in alkaline aqueous solutions, the effective  
33 electrophoretic mobility of the flavin analogue of interest has been measured with the  
34 residual substance. The  $pK_a$  values of the flavin analogues were analyzed through the  
35 changes in the effective electrophoretic mobility with varying pH of the separation  
36 buffer. One or two steps  $pK_a$  values were determined by the analysis. One of the  
37 degraded species from the flavin analogues, lumichrome, was also detected in the  
38 CZE analysis, and its  $pK_a$  values were also determined. While coexisting impurities  
39 generated over the storage conditions were found in some analogues, the  $pK_a$  values  
40 of the target analogues were successfully determined with the help of the CZE  
41 separations. A pressure-assisted CZE was utilized for the determination or the  
42 estimation of the  $pK_a$  values of such analogues as possessing carboxylic acid moiety.

## 43 **1 Introduction**

44 Redox reactions are essential on organic syntheses, and molecular catalysts inducing  
45 redox reactions are intensively investigated. For example, flavin analogues contain  
46 heterocyclic isoalloxazine (flavin, FL) ring and they are one of the famous redox-active  
47 molecular catalysts [1]. In nature, the heterocyclic isoalloxazine rings are utilized as  
48 an active center of the redox enzymes, in which xenobiotic substrates are metabolized  
49 through the oxidations such as dehydrogenation and monooxygenation. Thus, FL  
50 analogues are expected to work as oxidative molecular catalysts without any active  
51 center of metal ion [2-4]. On the activity design of the molecular catalysts, acid  
52 dissociation constant ( $pK_a$ ) is one of the key parameters. Since  $pK_a$  values and redox  
53 potentials are closely related to each other, experimentally determining the  $pK_a$  values  
54 of the FL analogues would be highly valuable on developing their redox catalysis.  
55 However, some of the FL analogues are not stable against light or alkaline base [5,6],  
56 which hampers the conventional methods for the  $pK_a$  determination.

57 Acid dissociation constants have classically been determined by potentiometric and  
58 spectrophotometric titrations. However, the homogeneous titrations are not applicable  
59 to such substances as are not pure or degradable. Spectrum shift is indispensable for

60 the  $pK_a$  determination by the spectrophotometric titration. On the contrary, CZE  
61 determination of acid dissociation constants is based on the changes in the effective  
62 electrophoretic mobility with protonation/deprotonation reaction under varying pH [7],  
63 and the CZE analysis is applicable to such substances as containing impurities or  
64 degradable under the measurement conditions [8-11]. Acid dissociation constants of  
65 alkaline-degradable phenolphthalein [8], labile drug compounds [9], acid-degradable  
66 tetrabromophenolphthalein ethyl ester [10], and heat-degradable bupropion [11] have  
67 been determined by utilizing the prominent characteristics of the CZE analysis.

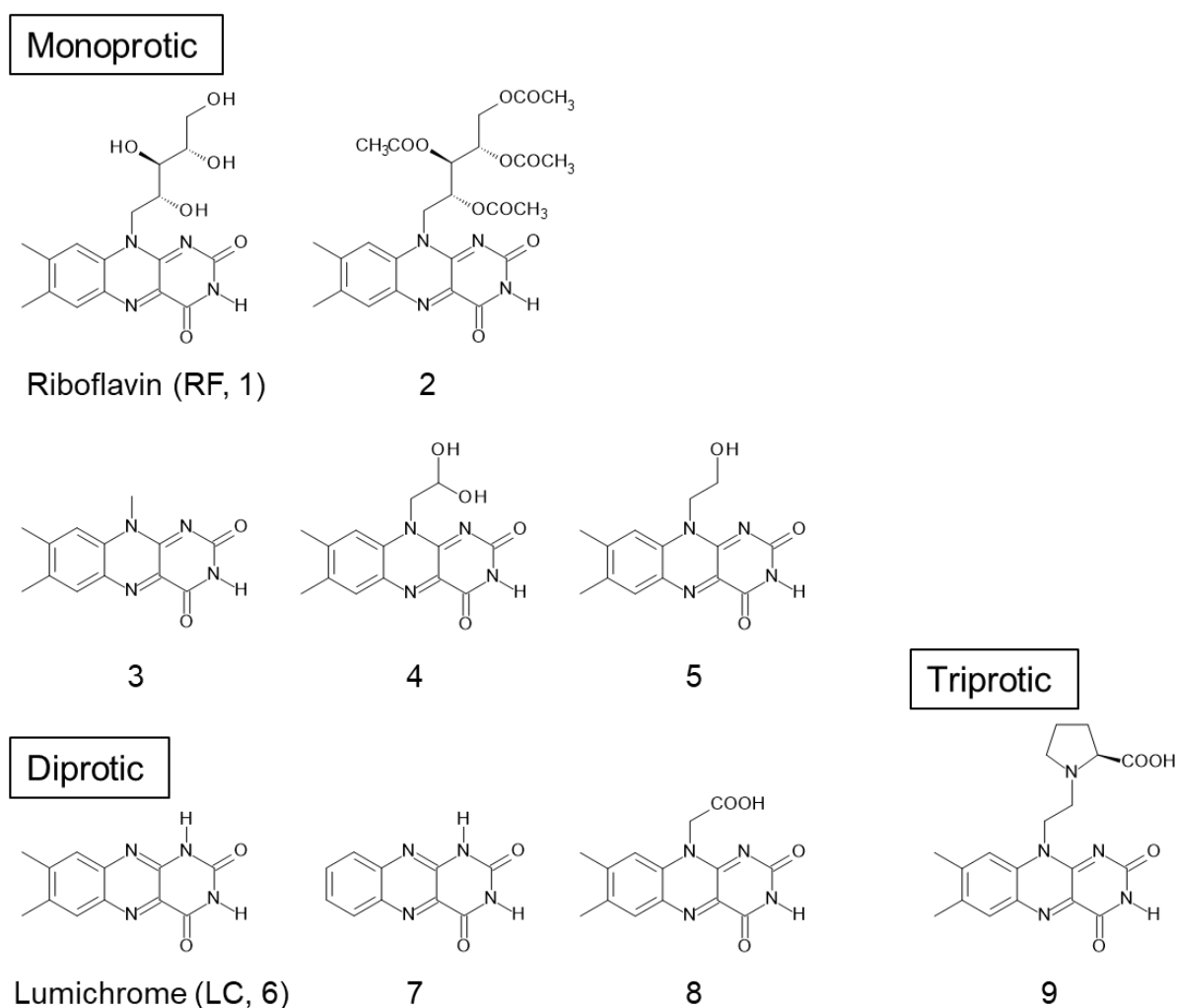
68 In this study, acid dissociation constants of 9 kinds of FL analogues were determined  
69 by CZE through the measurements of their effective electrophoretic mobility. Although  
70 some of the FL analogues were degradable under alkaline conditions and/or light  
71 exposure, the acid dissociation constants were successfully determined by CZE. Aim  
72 of this study is determining the  $pK_a$  values of such difficult substances, even though  
73 they are conditional values. The target analogue was resolved from the degraded  
74 species, and changes in the effective electrophoretic mobility of the analogue gave the  
75  $pK_a$  value(s). Some analogues contained unavoidable impurities formed under the  
76 storage conditions, the impurities were also resolved by CZE and the  $pK_a$  value(s) of  
77 the target analyte was also determined. Acid dissociation constants of the degraded  
78 species, as well as those of the impurities, were determined through the mobility  
79 change.

## 80 **2 Materials and methods**

### 81 **2.1 Chemicals**

82 Riboflavin and lumichrome, as well as all other reagents used for the synthesis of its  
83 analogues, were purchased from commercial supplies and used without further  
84 purification, besides *N*,3,4-trimethylaniline that was prepared according to the  
85 literature procedure [12]. Flavin analogues prepared and examined in this study are  
86 shown in Figure 1. They are categorized as monoprotic (5 analogues), diprotic (3  
87 analogues), and triprotic (1 analogue) acids. The analogues were synthesized  
88 according to the literature previously reported, and the details are written in Supporting  
89 Information. Separation buffers of the CZE were prepared with following buffer  
90 components: 0.010 mol L<sup>-1</sup> H<sub>3</sub>PO<sub>4</sub> – NaOH (pH 2.38 – 3.21); 0.010 mol L<sup>-1</sup> HCOOH

91 – NaOH (pH 3.13 – 3.53); 0.010 mol L<sup>-1</sup> CH<sub>3</sub>COOH – NaOH (pH 4.08 – 4.75); 0.010  
 92 mol L<sup>-1</sup> MES – NaOH (pH 5.48 – 6.42); 0.010 mol L<sup>-1</sup> HEPES – NaOH (pH 6.78 –  
 93 8.00); 0.010 mol L<sup>-1</sup> TAPS – NaOH (pH 8.02 – 9.28); 0.010 mol L<sup>-1</sup> CHES – NaOH  
 94 (pH 8.77 – 10.36); 0.010 mol L<sup>-1</sup> CAPS – NaOH (pH 9.88 – 11.27). NaOH was also  
 95 used in the alkaline pH conditions (pH 11.48 – 12.38). Ionic strength of the separation  
 96 buffers was adjusted at 0.010 mol L<sup>-1</sup> by adding adequate amount of NaCl. Internal  
 97 standards of naphthalene-1-sulfonate (1-NS<sup>-</sup>, sodium salt) and *N*-ethylquinolinium  
 98 (EtQ<sup>+</sup>, iodate salt) were from Tokyo Chemical Industry (Tokyo, Japan). Other reagents  
 99 were of analytical grade. Water used was purified by Milli-Q Gradient A10 (Merck-  
 100 Millipore, Milford, MA, USA).



101

102 **Figure 1.** Structures of flavin analogues examined in this study.

103

## 104 **2.2 Apparatus**

105 An Agilent Technologies (Waldbronn, Germany) <sup>3</sup>DCE was used for the CZE  
106 measurements equipped with a photodiode array detector. A fused silica capillary (GL  
107 Sciences, Tokyo, Japan) was set in a cassette cartridge, and the cartridge was  
108 installed in the CZE system. Dimensions of the capillary were 64.5 cm in total length,  
109 56 cm in the effective length from the sample injection point to the detection point, 50  
110  $\mu\text{m}$  in inner diameter and 375  $\mu\text{m}$  in outer diameter. A short capillary was also used in  
111 the pressure-assisted CZE at the acidic pH conditions; the total length and the  
112 effective length of the capillary were 48.5 cm and 40 cm, respectively.

113 A Waters (Milford, MA, USA) ACQUITY UPLC with LCT Premire XE was used as an  
114 LC-MS system; a reversed phase column of BEH C18 (Waters, 50 mm  $\times$  2.1 mm i.d.,  
115 1.7  $\mu\text{m}$ ) was attached to the LC-MS system. Flow rate of the eluent was set at 1 mL  
116  $\text{min}^{-1}$ , the MS polarity was ESI (+), and the injection volume was 20  $\mu\text{L}$ . JASCO (Tokyo,  
117 Japan) PU-2080 plus and UV-2075 plus were used as a conventional RP-HPLC  
118 system with UV detection. An RP column of Unison UK-C18 (75 mm length  $\times$  4.6 mm  
119 i.d., 3  $\mu\text{m}$  particle size; Imtakt, Kyoto, Japan) was attached to the system. An eluent of  
120 70/30 (v/v) water/ethanol was used. NMR spectra were recorded using JEOL (Tokyo,  
121 Japan) JNM-ECZ-400S (<sup>1</sup>H, 400 MHz). Chemical shifts are reported in ppm using TMS  
122 or the residual solvent peak as a reference. An HM-25G pH meter (TOA DKK, Tokyo,  
123 Japan) was used for the pH measurements of the separation buffers, after being  
124 calibrated daily with standard pH solutions. UV-LED light was used to expose and to  
125 degrade the FL analogues by NS375LIM (Emission maximum at 375 $\pm$ 5 nm, 1.4 W;  
126 Nitride Semiconductors, Naruto, Japan).

127

## 128 **2.3 Procedure**

129 Stock solutions of FL analogues were prepared as ethanol solution at  $\text{mmol L}^{-1}$  level.  
130 The stock solution was diluted with water, and a solution of an FL analogue was  
131 prepared at the concentration of about  $5 \times 10^{-5} \text{ mol L}^{-1}$ ; it was used as a sample  
132 solution for the CZE measurements. Monoanionic 1-NS<sup>-</sup> or monocationic EtQ<sup>+</sup> was  
133 added in the sample solution as an internal standard of the electrophoretic mobility.  
134 Ethanol at the concentration of 3 %(v/v) was also contained in the sample solution to  
135 monitor the electroosmotic flow (EOF). After the separation capillary being equilibrated

136 with a separation buffer, the sample solution was introduced into the capillary from the  
 137 anodic end by applying a pressure of 50 mbar for 5 s. Both ends of the capillary were  
 138 dipped in the separation buffer vials, and a DC voltage of 25 kV was applied for the  
 139 CZE. During the CZE, the capillary was thermostat at 25 °C by circulating a constant-  
 140 temperature air in the cassette cartridge. An analyte of the FL analogue and the  
 141 internal standard were photometrically detected at 220 nm. Effective electrophoretic  
 142 mobility,  $\mu_{\text{eff}}$ , was calculated with the migration times of the analyte and the EOF in an  
 143 ordinary manner. Acid dissociation constants of FL analogues were analyzed through  
 144 the change in  $\mu_{\text{eff}}$ , after standardized with the cationic or anionic internal standard.  
 145 On the measurements of the effective electrophoretic mobility at weakly acidic pH  
 146 conditions over 2.38 – 4.75, the velocity of electroosmotic flow was not fast enough,  
 147 and pressure-assisted CZE [13,14] was made. A constant pressure of 30 mbar was  
 148 applied to the inlet vial of the separation buffer during the electrophoresis.

149

## 150 **2.4 Determination of acid dissociation constants of FL analogues** 151 **by CZE**

152 Three types of the acid dissociation equilibria are included in the FL analogues of  
 153 monoprotic, diprotic, and triprotic acids. For monoprotic FL analogues, HA, the charge  
 154 changes from 0 to  $-1$  by the one-step acid dissociation reaction of the imide moiety.  
 155 The equilibrium reaction and its acid dissociation constant are written as in Eqs. (1)  
 156 and (2), respectively. Fractions of the species are related with the effective  
 157 electrophoretic mobility of the analogue,  $\mu_{\text{eff}}$ , and the  $\mu_{\text{eff}}$  value at a particular pH  
 158 condition is given in Eq. (3).



$$160 K_a = \frac{[\text{H}^+][\text{A}^-]}{[\text{HA}]} \quad (2)$$

$$161 \mu_{\text{eff}} = \frac{[\text{A}^-] \times \mu_{\text{ep,A}}}{[\text{HA}] + [\text{A}^-]} = \frac{10^{-\text{p}K_a} \times \mu_{\text{ep,A}}}{10^{-\text{pH}} + 10^{-\text{p}K_a}} \quad (3)$$

162 In Eq. (2),  $[\text{H}^+]$  is conventionally used instead of  $a_{\text{H}^+}$ , and  $K_a$  written in Eq. (2) is exactly  
 163 a mixed equilibrium constant. Value of  $\mu_{\text{ep,A}}$  is the electrophoretic mobility of the  
 164 monoanionic FL species. The protonated FL species, HA, is neutral, and its  
 165 electrophoretic mobility can be set as zero; Eq. (3) is thus given. A series of the pairs  
 166 of pH and  $\mu_{\text{eff}}$  value were put in Eq. (3), and the values of  $\mu_{\text{ep,A}}$  and  $\text{p}K_a$  were optimized

167 by a non-linear least-squares analysis [8,10]. Since the measured electrophoretic  
 168 mobility may deviate under the variation of experimental conditions, the value of  $\mu_{\text{eff}}$   
 169 was standardized with the electrophoretic mobility of 1-NS<sup>-</sup>,  $\mu_{\text{eff},1\text{-NS}}$ , and the  
 170 standardized value of  $\mu_{\text{eff}} / \mu_{\text{eff},1\text{-NS}}$  was used for the analysis. Because 1-NS<sup>-</sup> is a  
 171 monoanion over the wide pH range and its electrophoretic mobility is essentially  
 172 identical under the experimental conditions, and it was chosen as an internal standard.  
 173 On analyzing the  $\text{p}K_{\text{a}}$  value, a software of R program (Ver. 3.6.2) was used on the  
 174 basis of nonlinear least-squares regression [15]. Higher ionic strength would bias the  
 175  $\text{p}K_{\text{a}}$  value from its thermodynamic one,  $\text{p}K_{\text{a}}^{\circ}$ . However, the  $\text{p}K_{\text{a}}$  variation is generally  
 176  $\sim 0.1$  for monoprotic acid at ionic strength of 0.10 mol L<sup>-1</sup>. The  $\text{p}K_{\text{a}}$  values are  
 177 determined at ionic strength of 0.010 mol L<sup>-1</sup>, and the values determined in this study  
 178 would differ little from the thermodynamic ones; less than 0.1.

179 For diprotic FL analogues, H<sub>2</sub>A, the charge changes from 0 to -2 by the two-steps acid  
 180 dissociation reactions as in Eq. (4). The stepwise acid dissociation constants,  $K_{\text{a}1}$  and  
 181  $K_{\text{a}2}$ , are written in Eq. (5). The effective electrophoretic mobility of an FL analogue at  
 182 a particular pH condition is given in Eq. (6).



$$184 \quad K_{\text{a}1} = \frac{[\text{H}^+][\text{HA}^-]}{[\text{H}_2\text{A}]}, \quad K_{\text{a}2} = \frac{[\text{H}^+][\text{A}^{2-}]}{[\text{HA}^-]} \quad (5)$$

$$185 \quad \mu_{\text{eff}} = \frac{[\text{HA}^-] \times \mu_{\text{ep,HA}} + [\text{A}^{2-}] \times 2\mu_{\text{ep,HA}}}{[\text{H}_2\text{A}] + [\text{HA}^-] + [\text{A}^{2-}]} = \frac{10^{-\text{pH}-\text{p}K_{\text{a}1}} \times \mu_{\text{ep,HA}} + 10^{-\text{p}K_{\text{a}1}-\text{p}K_{\text{a}2}} \times 2\mu_{\text{ep,HA}}}{10^{-2\text{pH}} + 10^{-\text{pH}-\text{p}K_{\text{a}1}} + 10^{-\text{p}K_{\text{a}1}-\text{p}K_{\text{a}2}}} \quad (6)$$

186 Value of  $\mu_{\text{ep,HA}}$  is the electrophoretic mobility of the monoanionic FL species. The  
 187 electrophoretic mobility of dianionic FL species is assumed to be twice to the  
 188 monoanionic FL species [8,16]. A series of the pairs of pH and  $\mu_{\text{eff}}$  were put in Eq. (6),  
 189 and the values of  $\text{p}K_{\text{a}1}$  and  $\text{p}K_{\text{a}2}$ , as well as  $\mu_{\text{ep,HA}}$ , were optimized by a non-linear  
 190 least-squares analysis in a similar manner to the analysis of the one-step  $\text{p}K_{\text{a}}$  [16].

### 191 3 Results and discussion

#### 192 3.1 Determination of an acid dissociation constant of RF

193 Prior to the determination of the synthesized FL analogues, an acid dissociation  
 194 constant of RF was determined through the changes in the effective electrophoretic  
 195 mobility in CZE. Riboflavin is a monoprotic acid, and its charge changes from 0 to -1

196 by the acid dissociation reaction of the imide moiety. Electropherograms of RF at  
 197 several pH conditions are shown in Fig. S1 A. The migration time of RF got longer with  
 198 the increase in pH, suggesting that RF is more anionic at alkaline pH conditions.  
 199 Changes in the standardized electrophoretic mobility of RF are shown in Fig. S1 B.  
 200 Analysis of the results with Eq. (3) gave a  $pK_a$  value of  $10.29 \pm 0.06$  (mean  $\pm$  standard  
 201 error) by a least-squares analysis. The result agrees with the reported  $pK_a$  value of  
 202 10.2 [17]. The  $pK_a$  values are summarized in Table 1.

203

204 **Table 1.** Acid dissociation constants of RF and its photo-degradant of LC

	$pK_{a1}$ (this study) <sup>a)</sup>	$pK_{a2}$ (this study) <sup>a)</sup>	$pK_{a1}$ (ref.)	$pK_{a2}$ (ref.)
RF, 1	$10.29 \pm 0.06$ $10.24 \pm 0.03$ <sup>b)</sup>	N/A <sup>c)</sup>	$10.2$ <sup>d)</sup> $10.64$ <sup>e)</sup>	N/A
LC, 6	$8.36 \pm 0.02$ (degradant)	$(13.54 \pm 0.10)$ <sup>f)</sup>	$8.2$ <sup>g)</sup>	$11.4$ <sup>g)</sup>

205 <sup>a)</sup> Error: standard error.

206 <sup>b)</sup> Determined under the degraded conditions.

207 <sup>c)</sup> Not applicable.

208 <sup>d)</sup> Ref. 17.

209 <sup>e)</sup> Ref. 19. Determined by spectrophotometric titration.

210 <sup>f)</sup> Estimated value by extrapolation.

211 <sup>g)</sup> Ref. 18.

212

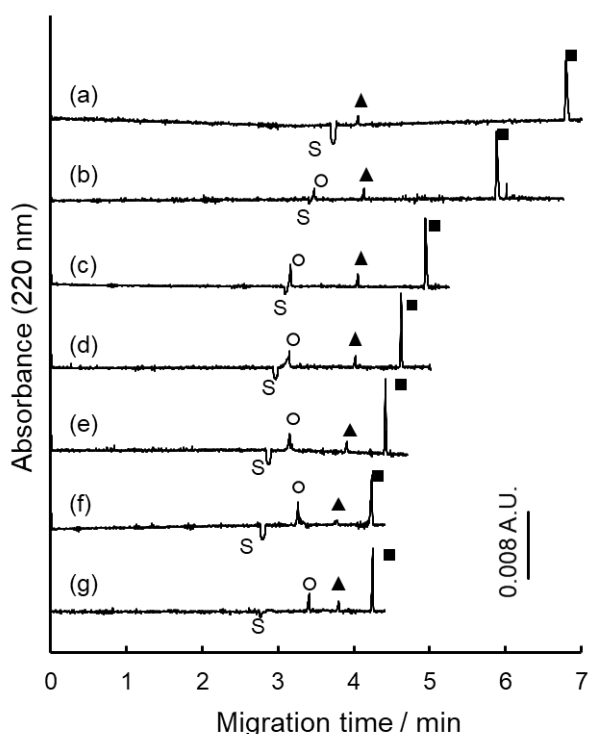
213 It is known that RF is degradable by light-exposure to form LC [5]. When the UV light  
 214 was irradiated to an aliquot of 3 mL RF solution containing  $1.0 \times 10^{-4}$  mol L<sup>-1</sup> RF, a CZE  
 215 determination of RF suggested that the residual RF gradually decreased with the  
 216 irradiation time and that the residual concentration of RF was about 60 % by the 120  
 217 min irradiation. Another distinct peak-signal was detected in the electropherograms  
 218 with the irradiated solution, and the signal intensity complementary increased along  
 219 with the decrease in the RF concentration. Therefore, the peak signal would be  
 220 attributed to a degraded substance. The photo-degraded solution was analyzed by a  
 221 conventional RP-HPLC and the LC-MS. The retention time of a degradant was about  
 222 20 min in the RP-HPLC, while that of RF was about 5 min. A mass number of 243.09  
 223 was detected by LC-MS with the substance of the longer retention time; it is attributed  
 224 to protonated LC.

225 The acid dissociation constant of RF was also determined under the degraded  
 226 conditions. An aliquot of aqueous RF solution at the concentration of  $5 \times 10^{-4}$  mol L<sup>-1</sup>  
 227 was exposed under a UV lamp for 120 min, and the solution was diluted by 10 times



228 and used for the  $pK_a$  determination after adding  $2 \times 10^{-5} \text{ mol L}^{-1}$  1-NS<sup>-</sup> as an internal  
229 standard and 3 % (v/v) ethanol as an EOF marker. Electropherograms of the degraded  
230 RF are shown in Figure 2; the residual RF (open circle) is still detected with the  
231 degraded solution. It can be noticed that additional peak indicated with the filled  
232 triangle is also detected in the electropherograms, as mentioned above. The migration  
233 time of RF, as well as that of the degradant, got longer with increasing pH of the  
234 separation buffer; both RF and the degradant become more anionic.

235



236

237 **Figure 2.** Electropherograms of RF at several  
238 pH conditions after UV-light exposure for 120  
239 min. pH conditions: (a), 7.82; (b), 8.45; (c),  
240 9.05; (d), 9.70; (e), 10.12; (f), 10.77; and (g),  
241 11.48. Symbols: ○, RF; ▲, LC as a degradant  
242 from RF; ■, 1-NS; S, solvent (EOF). Sample  
243 solution:  $5 \times 10^{-5} \text{ mol L}^{-1}$  RF (partly degraded) +  
244  $2 \times 10^{-5} \text{ mol L}^{-1}$  1-NS<sup>-</sup> (I.S.) + 3 % (v/v) ethanol.  
245 Separation buffers are written in the text. CZE  
246 conditions: applied voltage, 25 kV; sample  
247 injection, 50 mbar  $\times$  5 s; detection wavelength,  
248 220 nm; capillary temperature, 25 °C.

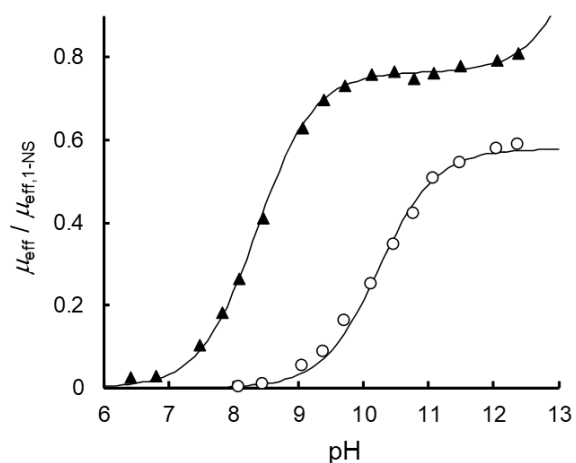
249

250 Changes in the effective electrophoretic mobility,  $\mu_{\text{eff}}$ , are shown in Figure 3 after  
251 standardized with  $\mu_{\text{eff},1\text{-NS}}$ . The standardized  $\mu_{\text{eff}}$  of the monoanionic degradant at pH  
252 around 11 is larger than RF, and the degradant would possess lighter molecular mass

253 than RF. While RF showed monoprotic profile of the mobility change, the  $\mu_{\text{eff}}$  of the  
254 degradant tended to increase at the alkaline pH conditions over 12. The acid  
255 dissociation constant of RF under the degraded conditions was also determined with  
256 Eq. (3), and  $pK_a$  value of  $10.24 \pm 0.03$  was obtained (Table 1). The  $pK_a$  value agreed  
257 with the freshly prepared RF solution, as well as the reference value [17]. Therefore,  
258 usefulness of the CZE analysis, electrophoretic separation of the target analyte from  
259 coexisting substances [8-11], was also demonstrated in this study.

260 Acid dissociation constants of the degradant were also determined through the  
261 changes in the effective electrophoretic mobility. The increased  $\mu_{\text{eff}}$  value at the  
262 alkaline pH conditions suggested the formation of a dianionic species. The CZE  
263 measurements, however, are limited under the pH conditions below  $\sim 12$ , because the  
264 higher pH conditions accompany the high salt concentrations, yielding much Joule's  
265 heat and temperature increase. Since the dianionic species is twice in its charge from  
266 the monoanionic species and its molecular mass is almost identical to the monoanionic  
267 species,  $\mu_{\text{eff}}$  value of the dianionic species is supposed to be twice to the monoanionic  
268 species. This assumption was valid in phenolphthalein [8] and fluorescein derivatives  
269 [16]. Equation (6) was thus used for the determination of the two steps of the  $pK_a$   
270 values;  $pK_{a1} = 8.36 \pm 0.02$  and  $pK_{a2} = 13.54 \pm 0.10$  were obtained by the least-squares  
271 analysis. It should be taken care of that the  $pK_{a2}$  value obtained in this study is the  
272 results of the extrapolated analysis. The  $pK_{a1}$  value obtained in this study agreed well  
273 with the reported value of LC ( $pK_{a1} = 8.2$ ) [18], and the degradant detected in this study  
274 would be LC. Lumichrome is diprotic acid with the imide moiety and N(1)-H [18], and  
275 two steps of the mobility change would also suggest the degradant to be LC. Therefore,  
276 another usefulness of the CZE analysis is also demonstrated in this study; the  
277 degradant can directly be analyzed without any isolation from the reaction mixture. On  
278 the other hand, the  $pK_{a2}$  value obtained in this study did not agree with the reported  
279 value of 11.4 [18]. The  $\mu_{\text{eff}}$  value of the degradant LC slightly changed at the pH  
280 conditions at around 11, suggesting the lack of the acid dissociation equilibrium at this  
281 pH range; the reference value determined by a spectrophotometric titration would not  
282 be correct.

283



284

285 **Figure 3.** Changes in the effective  
 286 electrophoretic mobility of RF and LC as a  
 287 degradant from RF. The electrophoretic  
 288 mobility was standardized with 1-NS<sup>-</sup> as an  
 289 internal standard. Symbols:  $\circ$ , RF;  $\blacktriangle$ , LC as a  
 290 degradant. The curves are drawn with the  
 291 optimized results. The CZE conditions are the  
 292 same as in Fig. 2.

293

## 294 **3.2 Determination of acid dissociation constants of FL analogues** 295 **by CZE**

### 296 **3.2.1 Acid dissociation constant of FL analogue 2**

297 Riboflavin tetraacetate (FL analogue 2) is a monoprotic acid, and its charge changes  
 298 from 0 to -1 by the acid dissociation reaction of the imide moiety. Electropherograms  
 299 at several pH conditions are shown in Figure S2 A, and the changes in  $\mu_{\text{eff}}$  are shown  
 300 in Figure S2 B after standardized with  $\mu_{\text{eff},1\text{-NS}}$ . Analysis of the changes in  $\mu_{\text{eff}}$  with Eq.  
 301 (3) gave a  $\text{p}K_{\text{a}}$  value of  $10.21 \pm 0.05$ .

302 An adjacent peak was detected just after the FL analogue 2. A small portion of FL  
 303 analogue 2 would have hydrolyzed in the alkaline separation buffer during the CZE.  
 304 When FL analogue 2 at its concentration of  $1.0 \times 10^{-4} \text{ mol L}^{-1}$  was treated in an alkaline  
 305 solution of  $5 \times 10^{-4} \text{ mol L}^{-1}$  NaOH for 50 min, additional peak signal was detected by  
 306 CZE as an adjacent peak behind to the peak signal of FL analogue 2. Thus, the newly  
 307 detected signal would be attributed to the hydrolyzed species of FL analogue 2; one  
 308 or more ester moieties are hydrolyzed to form alcohol group(s). Even under the  
 309 alkaline-degraded conditions, the acid dissociation constant of FL analogue 2 was

310 successfully determined as  $pK_a = 10.24 \pm 0.04$ . The  $pK_a$  value is close to the one  
311 determined with the freshly prepared solution.

312 The alkaline-treated FL analogue 2 solution was analyzed by RP-HPLC and LC-MS.  
313 A certain number (~10) of peaks were detected by a conventional RP-HPLC-UV  
314 detected at 220 nm. The LC-MS chromatograms are shown in Figure S3. The mass  
315 numbers detected by the LC-MS were 545.188 (FL analogue 2 +H), 503.178, 419.157,  
316 and 377.146. The Each mass number corresponds to deacetylated substances from  
317 FL analogue 2, and the mass number 377.146 is equivalent to RF. Therefore, the  
318 newly detected peaks in Figure S2 would be attributed to the hydrolyzed substances  
319 from FL analogue 2.

320

### 321 **3.2.2 Acid dissociation constant of FL analogue 3**

322 Lumiflavin (FL analogue 3) is also a monoprotic acid, and its charge similarly changes  
323 from 0 to -1 by the acid dissociation reaction of the imide moiety. Electropherograms  
324 are shown in Figure S4 A, and the changes in  $\mu_{\text{eff}}$  are shown in Figure S4 B after  
325 standardized with  $\mu_{\text{eff},1-\text{NS}}$ . An additional peak signal indicated with filled triangle was  
326 detected with FL analogue 3; it would be attributed to an impurity formed under the  
327 storage conditions. An additional peak was also detected with the FL analogue 3  
328 solution by a conventional RP-HPLC-UV detection; LC-MS analysis gave a substance  
329 of mass number of 243.09. The mass number is equivalent to LC, and the impurity  
330 would be LC. The migration time of FL analogue 3, as well as the additional peak  
331 signal, got longer than the EOF with the increase in pH as in the case of RF. Analysis  
332 of the changes in  $\mu_{\text{eff}}$  of FL analogue 3 with Eq. (3) gave a  $pK_a$  value of  $10.38 \pm 0.04$ .  
333 Unfortunately, the additional peak was not detected in the alkaline separation buffer,  
334 it would have been overlapped with FL analogue 3. The monoprotic behavior of the  
335 additional peak was analyzed with Eq. (3), and a  $pK_a$  value of  $8.29 \pm 0.02$  was obtained;  
336 the  $pK_a$  value is close to that of LC. The usefulness of the CZE analysis is also  
337 demonstrated with such substance as containing impurity, as well as the  $pK_a$  analysis  
338 of the impurity.

339

### 340 **3.2.3 Acid dissociation constant of FL analogue 4**

341 10-(2,2-Dihydroxyethyl)-7,8-dimethylisoalloxazine (FL analogue 4) is also a  
342 monoprotic acid, and its charge changes from 0 to  $-1$  by the acid dissociation reaction  
343 of the imide moiety. Electropherograms are shown in Figure S5 A, and the changes in  
344  $\mu_{\text{eff}}$  are shown in Figure S5 B after standardized with  $\mu_{\text{eff},1-\text{NS}}$ . A peak signal  
345 corresponding to FL analogue 4 disappeared at pH 12.05 (Figure S5 A(f)). The result  
346 suggests that FL analogue 4 has decomposed at the alkaline conditions. An additional  
347 peak signal indicated with filled triangle was also detected with FL analogue 4 as in  
348 the case of FL analogue 3. Although the migration time of the EOF became faster at  
349 alkaline pH conditions, the peak signal of FL analogue 4 much delayed from the EOF  
350 at alkaline pH conditions. Analysis of the changes in  $\mu_{\text{eff}}$  with Eq. (3) gave a  $pK_a$  value  
351 of  $10.22 \pm 0.08$  for FL analogue 4. An acid dissociation constant of the impurity was  
352 also determined with Eq. (3), and a  $pK_a$  value of  $8.40 \pm 0.02$  was obtained. LC-MS  
353 analysis gave a mass number of 243.09, and the impurity was also found to be LC.

354

### 355 **3.2.4 Acid dissociation constant of FL analogue 5**

356 10-(2-Hydroxyethyl)-7,8-dimethylisoalloxazine (FL analogue 5) is also a monoprotic  
357 acid, and its charge changes from 0 to  $-1$  by the acid dissociation reaction of the imide  
358 moiety. Electropherograms are shown in Figure S6 A, and the changes in  $\mu_{\text{eff}}$  are  
359 shown in Figure S6 B after standardized with  $\mu_{\text{eff},1-\text{NS}}$ . A peak signal corresponding to  
360 FL analogue 5 was detected. Although a peak signal of an impurity or the degradant  
361 was detected at pH around 10.5, it did not interfere with the  $pK_a$  analysis of FL  
362 analogue 5. The additional peak signal was not detected when FL analogue 5 was  
363 freshly prepared, and therefore, it would be generated under light exposure. The  
364 migration time of FL analogue 5 got longer than the EOF with the increase in pH as in  
365 the case of RF. Analysis of the changes in  $\mu_{\text{eff}}$  with Eq. (3) gave a  $pK_a$  value of  
366  $10.35 \pm 0.04$  for FL analogue 5.

367

### 368 **3.2.5 Acid dissociation constants of FL analogue 7**

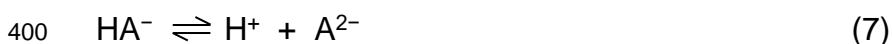
369 Alloxazine (FL analogue 7) is a diprotic acid, and its charge changes from 0 to  $-2$  by  
370 the acid dissociation reactions of the imide moiety and N(1)-H. Electropherograms are  
371 shown in Figure S7 A, and the changes in  $\mu_{\text{eff}}$  are shown in Figure S7 B after

372 standardized with  $\mu_{\text{eff},1-\text{NS}}$ . The  $\mu_{\text{eff}}$  value increased in the pH range from 7 to 9, and an  
 373 acid dissociation equilibrium is applied in this pH range. The  $\mu_{\text{eff}}$  value further  
 374 increased in the pH range over 11. This increase would be attributed to the 2nd step  
 375 of the deprotonation. Two steps of the acid dissociation equilibria are analyzed with  
 376 Eq. (6) in a similar manner to LC, and the  $pK_{\text{a}}$  values of  $pK_{\text{a}1} = 8.07 \pm 0.01$  and  $pK_{\text{a}2} =$   
 377  $12.96 \pm 0.4$  were obtained by the least-squares analysis. It should also be taken care  
 378 of that the  $pK_{\text{a}2}$  value obtained in this study is the results of the extrapolated analysis,  
 379 as in the case of LC. It can be noted that both  $pK_{\text{a}1}$  and  $pK_{\text{a}2}$  values of FL analogue 7  
 380 are smaller than those of LC. The result would be attributed to the lack of two methyl  
 381 groups of electron donating moiety.

382

### 383 3.2.6 Acid dissociation constants of FL analogue 8 at weakly alkaline pH region

384 7,8-Dimethyl-10-carboxymethylisalloxazine (FL analogue 8) is a diprotic acid, and its  
 385 charge changes from 0 to  $-2$  by the acid dissociation equilibria of a carboxylic acid  
 386 moiety and an imide moiety. The carboxylic acid moiety would dissociate at weakly  
 387 acidic pH region, and the imide moiety at weakly alkaline pH region.  
 388 Electropherograms in the neutral to weakly alkaline pH range are shown in Figure S8,  
 389 and the changes in  $\mu_{\text{eff}}$  are shown in Figure 4 A after standardized with  $\mu_{\text{eff},1-\text{NS}}$ . A peak  
 390 signal attributed to FL analogue 8, as well as an impurity, is detected in the  
 391 electropherograms. According to the presence of the carboxylate moiety, FL analogue  
 392 8 is anionic in the pH range between 7.9 and 12.0. On the other hand, detection of FL  
 393 analogue 8 was difficult at acidic pH conditions below 4.5, because the electroosmotic  
 394 flow was too slow at the acidic pH conditions to detect the anionic species. In Figure  
 395 4 A, the  $\mu_{\text{eff}}$  value of FL analogue 8 increased in the pH range at around 11, suggesting  
 396 that the charge changes from  $-1$  to  $-2$  in the pH range: the 2nd step of the  
 397 deprotonation. The acid dissociation equilibrium of  $K_{\text{a}2}$  is expressed as in Eq. (7) with  
 398 its acid dissociation constant (8). The effective electrophoretic mobility is contributed  
 399 from both charged species of  $\text{HA}^-$  and  $\text{A}^{2-}$ , and it is written as in Eq. (9).



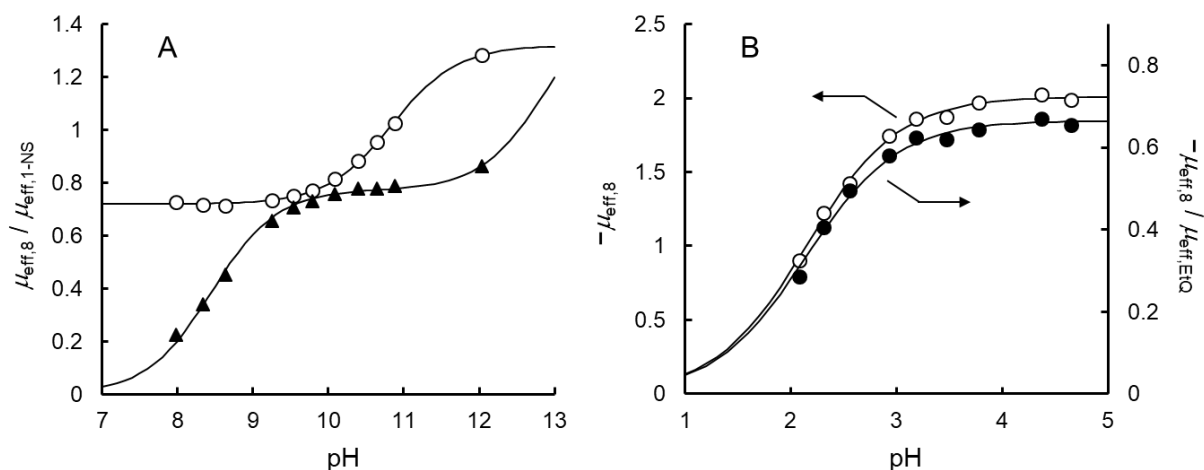
$$401 \quad K_{\text{a}2} = \frac{[\text{H}^+][\text{A}^{2-}]}{[\text{HA}^-]} \quad (8)$$

$$402 \quad \mu_{\text{eff}} = \frac{[\text{HA}^-] \times \mu_{\text{ep,HA}} + [\text{A}^{2-}] \times \mu_{\text{ep,A}}}{[\text{HA}^-] + [\text{A}^{2-}]} = \frac{10^{-\text{pH}} \times \mu_{\text{ep,HA}} + 10^{-\text{p}K_{\text{a}2}} \times \mu_{\text{ep,A}}}{10^{-\text{pH}} + 10^{-\text{p}K_{\text{a}2}}} \quad (9)$$

403

404 Values of  $\mu_{ep,HA}$  and  $\mu_{ep,A}$  are the electrophoretic mobility of the monoanionic and  
405 dianionic species, respectively. A series of the pairs of pH and  $\mu_{eff}$  were put in Eq. (9),  
406 and the values of  $\mu_{ep,HA}$ ,  $\mu_{ep,A}$  and  $pK_{a2}$  were optimized by a non-linear least-squares  
407 analysis in a similar manner after the standardization with 1-NS<sup>-</sup> as an internal  
408 standard. A  $pK_{a2}$  value of  $10.84 \pm 0.02$  was obtained by the analysis. Optimized values  
409 of standardized  $\mu_{ep,HA}$  and  $\mu_{ep,A}$  were 0.72 and 1.32, respectively. The standardized  
410  $\mu_{ep,A}$  value is 1.83 times to that of  $\mu_{ep,HA}$  value, and the twice charge of A<sup>2-</sup> against HA<sup>-</sup>  
411 would be appropriate. The effective electrophoretic mobility of the impurity showed  
412 two-steps increase (Figure 4 A), and the increase was also analyzed as two-steps acid  
413 dissociation equilibrium, as written in Eq. (6); acid dissociation constants of  $pK_{a1} =$   
414  $8.45 \pm 0.02$  and  $pK_{a2} = 12.91 \pm 0.09$  were determined by the analysis. An LC-MS  
415 analysis gave a mass number of 243.09, and the impurity was also LC.

416



417

418 **Figure 4.** Changes in the effective electrophoretic mobility of FL analogue 8. (A) At weakly  
419 alkaline conditions. The  $\mu_{eff}$  values are standardized with  $\mu_{eff,1-NS}$ .  $\circ$ , FL analogue 8;  $\blacktriangle$ , impurity.  
420 (B) At weakly acidic conditions.  $\circ$ , the  $\mu_{eff}$  values are directly used for the analysis;  $\bullet$ , the  $\mu_{eff}$   
421 values are used for the analysis after standardized with  $\mu_{eff,EtQ}$ . The curves are drawn with the  
422 optimized results. CZE conditions: (A), applied voltage, 25 kV; sample injection, 50 mbar  $\times$  5  
423 s; detection wavelength, 220 nm; capillary temperature, 25 °C; (B), pressure-assisted CZE  
424 under 25 kV applied voltage and 30 mbar pressure assist, other conditions are as in (A).

425

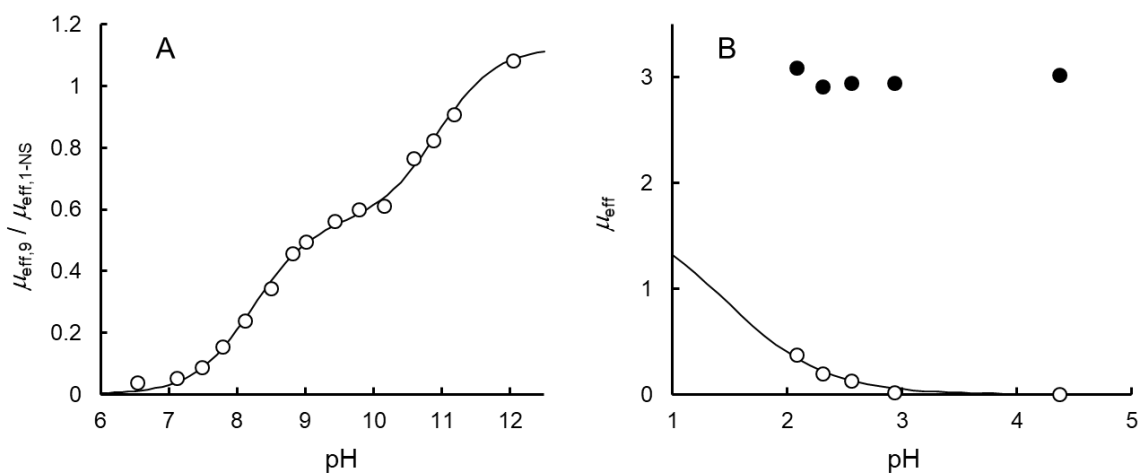
### 426 3.2.7 Acid dissociation constants of FL analogue 9 at weakly alkaline pH region

427 2-(7,8-Dimethyl-10-isoalloxazolyl)ethyl-L-proline (FL analogue 9) is a triprotic acid, and  
428 its charge changes from +1 to -2 by the three-steps acid dissociation reactions of a  
429 carboxylic acid moiety, a protonated pyrrolidine moiety, and an imide moiety.

430 Electropherograms are shown in Figure S9, and the changes in  $\mu_{\text{eff}}$  are shown in  
431 Figure 5 A after standardized with  $\mu_{\text{eff},1\text{-NS}}$ . The migration time of FL analogue 9 got  
432 longer than the EOF with the increase in pH. Two-steps increase in the  $\mu_{\text{eff}}$  is read out,  
433 and the acid dissociation constants of  $pK_{a2}$  (protonated pyrrolidine moiety) and  $pK_{a3}$   
434 (imide moiety) have been analyzed by Eq. (6) through the  $\mu_{\text{eff}}$  values;  $pK_{a2} = 8.23 \pm 0.04$   
435 and  $pK_{a3} = 10.93 \pm 0.06$  were determined. The  $pK_a$  values for the FL analogues  
436 determined by the CZE are summarized in Table 2.

437 An acid dissociation constant of FL analogue 9 was also determined by  
438 spectrophotometric titration at alkaline pH region. Changes in the absorbance at 356  
439 nm was used for the analysis. One step of the absorbance change was observed with  
440 a clear isosbestic point at 368 nm, and a  $pK_a$  value of  $10.74 \pm 0.02$  was determined.  
441 The  $pK_a$  value corresponds to the  $pK_{a3}$  value at the imide moiety determined by the  
442 CZE. However, the spectrum slightly changed in the pH range from 6.7 to 9.4 where  
443 the  $pK_{a2}$  value was determined by the CZE analysis. The absence of the spectrum  
444 shift by the acid dissociation equilibrium would be because of the pyrrolidine moiety  
445 being shielded from the resonance skeleton. Therefore, CZE analysis is applicable to  
446 such substance without any spectrum shift.

447



448

449 **Figure 5.** Changes in the effective electrophoretic mobility of FL analogue 9. (A) At weakly  
450 alkaline conditions.  $\circ$ , FL analogue 9 standardized with  $\mu_{\text{eff},1\text{-NS}}$ . (B) At weakly acidic conditions.  
451  $\circ$ , FL analogue 9;  $\bullet$ , EtQ<sup>+</sup>. The curves are drawn with the optimized results. CZE conditions:  
452 (A), applied voltage, 25 kV; sample injection, 50 mbar  $\times$  5 s; detection wavelength, 220 nm;  
453 capillary temperature, 25 °C; (B), pressure-assisted CZE under 25 kV applied voltage and 30  
454 mbar pressure assist, other conditions are as in (A).

455

456



457

**Table 2.** Acid dissociation constants of FL analogues determined in this study

	$pK_{a1}$ <sup>a)</sup>	$pK_{a2}$ <sup>a)</sup>	$pK_{a1}$ <sup>a)</sup>	Remark
Analogue 2	10.21±0.05 10.24±0.04 <sup>b)</sup>	N/A <sup>c)</sup>	N/A <sup>c)</sup>	Degraded at alkaline conditions: hydrolysis of ester moiety.
Analogue 3	10.38±0.04	N/A	N/A	Degraded at storage conditions: LC was formed.
Analogue 4	10.22±0.08	N/A	N/A	Degraded at alkaline conditions: LC was formed.
Analogue 5	10.35±0.04	N/A	N/A	Degraded at storage conditions with light exposure: LC was formed.
Analogue 7	8.07±0.01	(12.96±0.4) <sup>d)</sup>	N/A	Impurity of LC was contained.
Analogue 8	2.15±0.02 <sup>e)</sup>	10.84±0.02	N/A	
Analogue 9	(1.46±0.03) <sup>d),e)</sup>	8.23±0.04 (-) <sup>f)</sup>	10.93±0.06 (10.74±0.02) <sup>f)</sup>	

458

<sup>a)</sup> Error: standard error.

459

<sup>b)</sup> Degraded at alkaline conditions.

460

<sup>c)</sup> Not applicable.

461

<sup>d)</sup> Estimated value by extrapolation.

462

<sup>e)</sup> Determined by pressure-assisted CZE; no standardization of  $\mu_{eff}$ .

463

<sup>f)</sup> Determined by spectrophotometric titration.

464

### 465 3.3 Determination of acid dissociation constants of FL analogues

#### 466 by pressure-assisted CZE

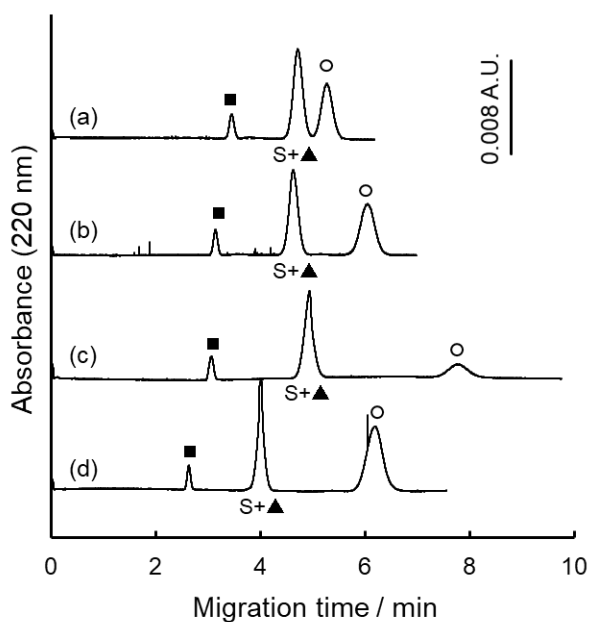
467 Acid dissociation constants of the carboxylic acid moiety on FL analogues 8 and 9  
 468 were difficult to analyze by CZE, because their peak signals were not detected at acidic  
 469 pH conditions due to the slow EOF. Therefore, pressure-assisted CZE [13,14] was  
 470 examined to compensate the slow EOF and to detect the analytes even at the acidic  
 471 pH conditions. An assisting air-pressure of 30 mbar was applied to the inlet vial during  
 472 the electrophoresis. The migration time of the EOF got faster and the analytes of  
 473 interest can be detected by the pressure-assisted CZE.

#### 474 3.3.1 Acid dissociation constant of FL analogue 8 at acidic pH region

475 As noted in the previous section, FL analogue 8 is electrically neutral at acidic pH  
 476 conditions and its charge changes from 0 to -1 by the acid dissociation reaction of the  
 477 carboxylic acid moiety. Pressure-assisted electropherograms are shown in Figure 6.  
 478 FL analogue 8 migrated slower than the EOF, and it is also anionic in this pH range.  
 479 The peak widths became wider by applying the pressure compared with the normal

480 CZE, because the analyte in the plug zone is dispersed by the parabolic flow in the  
 481 directions of both the tube axis and the tube diameter. However, the effective  
 482 electrophoretic mobility of the internal standard, EtQ<sup>+</sup>, was affected little by the  
 483 pressure, and therefore, the effective electrophoretic mobility of the analyte would be  
 484 measured properly, and it would be used for the pK<sub>a</sub> analysis. Changes in  $\mu_{\text{eff}}$  of FL  
 485 analogue 8 are shown in Figure 4 B; both directly measured  $\mu_{\text{eff}}$  values and  
 486 standardized  $\mu_{\text{eff}}$  values with EtQ<sup>+</sup> were used for the analysis. Since anionic internal  
 487 standard of 1-NS<sup>-</sup> was not detected even by the pressure-assisted CE, cationic EtQ<sup>+</sup>  
 488 was used for the standardization. Fortunately, protonated species of FL analogue 8 is  
 489 electrically neutral, its electrophoretic mobility is zero and Eq. (3) was used for the  
 490 analysis on the basis of an acid dissociation equilibrium (1). A pK<sub>a1</sub> value of 2.15±0.02  
 491 was obtained with the direct analysis of  $\mu_{\text{eff}}$  values, whereas a pK<sub>a1</sub> value of 2.14±0.03  
 492 was obtained after the standardization with EtQ<sup>+</sup>. Therefore, the standardization  
 493 worked well.

494



495

496 **Figure 6.** Electropherograms of FL analogue 8  
 497 at acidic pH conditions by the pressure-  
 498 assisted CZE. pH conditions: (a), 2.08; (b),  
 499 2.56; (c), 3.47; (d), 4.65. Symbols: o, FL  
 500 analogue 8; ▲, LC as a degradant; ■, EtQ<sup>+</sup>; S,  
 501 solvent (EOF). Sample solution: 6×10<sup>-5</sup> mol L<sup>-1</sup>  
 502 FL analogue 8 + 3×10<sup>-5</sup> mol L<sup>-1</sup> EtQ<sup>+</sup> (I.S.) +  
 503 3 % (v/v) ethanol. Separation buffers are written  
 504 in the text. CZE conditions: applied voltage, 25  
 505 kV; assist pressure, 30 mbar; sample injection,

506 50 mbar × 5 s; detection wavelength, 220 nm;  
507 capillary temperature, 25 °C.

508

### 509 **3.3.2 Acid dissociation constants of FL analogue 9 at acidic pH region**

510 An acid dissociation constant of FL analogue 9 was also examined by the pressure-  
511 assisted CZE. Its charge changes from +1 to 0 by the acid dissociation reaction of the  
512 carboxylic acid moiety, and the dissociated species is zwitterion. Electropherograms  
513 are shown in Figure 7; broad peaks are also detected as in the case of FL analogue  
514 8. It can be seen from Figure 7 that FL analogue 9 migrated faster than the EOF at  
515 acidic pH conditions and it is cationic. Although only a broad peak is detected the EOF  
516 position at pH 2.56 (b), the broad peak was found to be composed of two overlapped  
517 peaks of FL analogue 9 and the EOF when detected at 254 nm. Changes in the  
518 electrophoretic mobility are shown in Figure 5 B. FL analogue 9 becomes more  
519 cationic at acidic conditions. Different from FL analogue 8, the electrophoretic mobility  
520 of the protonated species of  $H_3A^+$  is not zero, and the value is difficult to measure. The  
521 acid dissociation equilibrium and its acid dissociation constant are written as in Eq.  
522 (10) and (11), respectively. The effective electrophoretic mobility is contributed from  
523 the positively charged species,  $H_3A^+$ , and it is given in Eq. (12).

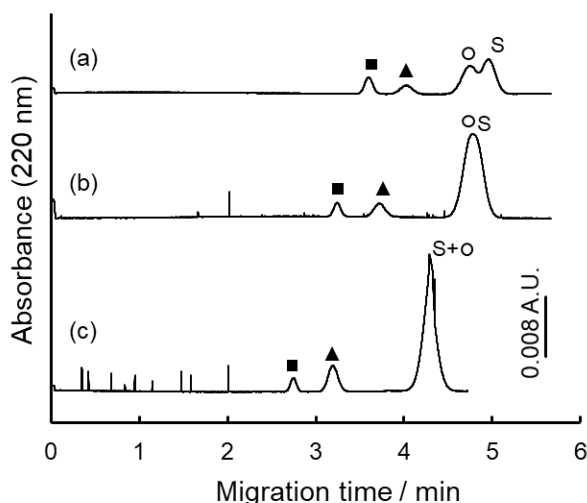


$$525 \quad K_a = \frac{[H^+][H_2A]}{[H_3A^+]} \quad (11)$$

$$526 \quad \mu_{\text{eff}} = \frac{[H_3A^+] \times \mu_{\text{ep,H3A}}}{[H_3A^+] + [H_2A]} = \frac{10^{-\text{pH}} \times \mu_{\text{ep,H3A}}}{10^{-\text{pH}} + 10^{-\text{p}K_a}} \quad (12)$$

527 Value of  $\mu_{\text{ep,H3A}}$  is the electrophoretic mobility of the monocationic species. Another  
528 problem is that CZE measurements at pH conditions below 2 is also difficult owing to  
529 the high salt concentrations and the generated Joule's heat. To estimate the acid  
530 dissociation constant of the carboxylic acid moiety of FL analogue 9, the  
531 electrophoretic mobility of the cationic species of +1 charged one was assumed to be  
532 equal to that of the anionic species of -1 charged one. An acid dissociation constant  
533 of  $1.46 \pm 0.03$  was estimated under such assumption.

534



535

536 **Figure 7.** Electropherograms of FL analogue 9  
 537 at acidic pH conditions by pressure-assisted  
 538 CZE. pH conditions: (a), 2.08; (b), 2.56; (c),  
 539 4.37. Symbols: ○, FL analogue 9; ▲, impurity;  
 540 ■, EtQ<sup>+</sup>; S, solvent (EOF). Sample solution:  
 541  $6 \times 10^{-5} \text{ mol L}^{-1}$  FL analogue 9 +  $3 \times 10^{-5} \text{ mol L}^{-1}$   
 542 EtQ<sup>+</sup> (I.S.) + 3 % (v/v) ethanol. Separation  
 543 buffers are written in the text. CZE conditions:  
 544 applied voltage, 25 kV; assist pressure, 30  
 545 mbar; sample injection, 50 mbar × 5 s;  
 546 detection wavelength, 220 nm; capillary  
 547 temperature, 25 °C.

#### 548 **4 Concluding remarks**

549 In this study, acid dissociation constants were determined by CZE for a series of  
 550 molecular catalyst candidates of FL analogues. Changes in the  $\mu_{\text{eff}}$  by the protonation  
 551 or deprotonation were used for the CZE analysis. The CZE analysis was proved to be  
 552 useful for the separation of the target analyte from the coexisting substances including  
 553 degraded species and impurities. The CZE analysis is also applicable to such  
 554 substances as without spectrum shift. Pressure-assisted CZE was also utilized for the  
 555 measurements of the effective electrophoretic mobility at weakly acidic pH conditions,  
 556 where the electroosmotic flow is slow.

#### 557 **Acknowledgements**

558 This work was supported by a Grant-in-Aid for Scientific Research (C) (No. 17K05903)  
 559 from the Japan Society for the Promotion of Sciences (JSPS). The authors  
 560 acknowledge to Dr. Shoko Ueta (Tokushima University) for the LC-MS measurements.

561 **Conflict of interest**

562 The authors have declared no conflict of interest.

563 **5 References**

564 [1] Iida, H., Imada, Y., Murahashi, S.-I., *Org. Biomol. Chem.* 2015, 13, 7599-7613.

565 [2] Tagami, T., Arakawa, Y., Minagawa, K., Imada, Y., *Org. Lett.* 2019, 21, 6978-6982.

566 [3] Imada, Y., Kitagawa, T., Ohno, T., Iida, H., Naota, T., *Org. Lett.* 2010, 12, 32-35.

567 [4] Arakawa, Y., Yamanomoto, K., Kita, H., Minagawa, K., Tanaka, M., Haraguchi, N.,  
568 Itsuno, S., Imada, Y., *Chem. Sci.* 2017, 8, 5468-5475.

569 [5] Sheraz, M. A., Kazi, S. H., Ahmed, S., Anwar, Z., Ahmad, I., *Beilstein J. Org. Chem.*  
570 2014, 10, 1999-2012.

571 [6] Stanojević, J. S., Zvezdanović, J. B., Marković, D. Z., *Monatsh. Chem.* 2015, 146,  
572 1787-1794.

573 [7] Andradi, M., Buglyo, P., Zekany, L., Gaspar, A., *J. Pharm. Biomed. Anal.* 2007, 44,  
574 1040-1047.

575 [8] Takayanagi, T., Motomizu, S., *Chem. Lett.* 2001, 30, 14-15.

576 [9] Örnskov, E., Linusson, A., Folestad, S., *J. Pharm. Biomed. Anal.* 2003, 33, 379-  
577 391.

578 [10] Takayanagi, T., Tabara, A., Kaneta, T., *Anal. Sci.* 2013, 29, 547-552.

579 [11] Takayanagi, T., Itoh, D., Mizuguchi, H., *Chromatography* 2016, 37, 105-109.

580 [12] Imada, Y., Iida, H., Ono, S., Masui, Y., Murahashi, S.-I., *Chem. Asian J.* 2006, 1,  
581 136-147.

582 [13] Wang, J. L., Xu, X. J., Chen, D. Y., *J. Pharm. Biomed. Anal.* 2014, 88, 22-26.

583 [14] Konášová, R., Dyrtrtová, J. J., Kašička, V., *J. Chromatogr. A* 2015, 1408, 243-249.

584 [15] The R Project for Statistical Computing, <https://www.r-project.org/>.

585 [16] Hirabayashi, K., Hanaoka, K., Takayanagi, T., Toki, Y., Egawa, T., Kamiya, M.,  
586 Komatsu, T., Ueno, T., Terai, T., Yoshida, K., Uchiyama, M., Nagano, T., Urano, Y.,  
587 *Anal. Chem.* 2015, 87, 9061-9069.

588 [17] O'Neil, M. J. (Ed.), *The Merck Index 14th Ed.*, Merck Research Laboratories,  
589 Whitehouse Station, NJ 2006, p. 1413.

590 [18] Prukala, D., Sikorska, E., Koput, J., Khmelinskii, I., Karolczak, J., Gierszewski, M.,  
591 Sikorski, M., J. Phys. Chem. A 2012, 116, 7474-7490.

592 [19] Ghasemi, J., Ghobadi, S., Abbasi, B., Kubista, M., J. Kor. Chem. Soc. 2005, 49,  
593 269-277.

594

## 595 **Supporting information**

596 **Supporting information file:** Syntheses of FL analogues 2, 3, 4, 5, 7, 8, and 9 are  
597 described. Typical electropherograms and the changes in the effective mobility are  
598 shown in Figures S1, S2, S4, S5, S6, and S7 for FL analogues 1, 2, 3, 4, 5, and 7,  
599 respectively. Typical electropherograms are shown in Figures S8 and S9 for FL  
600 analogues 8 and 9, respectively. LC-MS chromatograms for alkaline-treated FL  
601 analogues 2 are shown in Figure S3.

602